PHYSICS AND CHEMISTRY OF SOLID STATE
V. 26, No. 3 (2025) pp. 532-540
Section: Technology

DOI: 10.15330/pcss.26.3.532-540

Vasyl Stefanyk Carpathian National University

ФІЗИКА І ХІМІЯ ТВЕРДОГО ТІЛА
Т. 26, № 3 (2025) С. 532-540
Технічні науки

PACS: 81.20.Ka

ISSN 1729-4428 (Print)
ISSN 2309-8589 (Online)

Thi My Anh Nguyen, Thanh Sinh Do, Thai Thinh Le, Thi Kim Xuan Nguyen, Cong Danh Nguyen, Nhi Kieu Vo, Ngoc Tuan Anh Mai

High-purity nano hydroxyapatite (CaP) synthesized at low temperature (<100°C): a promising candidate for large-scale production of nano fertilizers

Research Laboratories of Sai Gon Hi-Tech Park, Thu Duc City, Ho Chi Minh City, Vietnam, ntmanh.shtp@tphcm.gov.v

Calcium phosphate (CaP) nanoliquid fertilizers have shown great potential in improving nutrient uptake efficiency by providing a controlled and sustained release of calcium (Ca) and phosphate (P) ions. In this study, we successfully synthesized highly pure calcium phosphate nanoparticles with a uniform size of a few tens of nanometers using a simple and cost-effective method. By incorporating triethanolamine (TEA) as a complexing and stabilizing agent, we significantly reduced the synthesis temperature, leading to lower energy consumption and production costs while ensuring excellent nanoparticle quality. The resulting nano-hydroxyapatite ($Ca_{10}(PO_4)_6(OH)_2$) exhibited a high surface area, promoting gradual nutrient release and improved bioavailability for crops. This straightforward approach offers a scalable and economically viable route for producing advanced nanofertilizers tailored for sustainable agriculture.

Keywords: Nano-hydroxyapatite (CaP); Nanofertilizer; Low-temperature synthesis; Triethanolamine (TEA); Sustainable agriculture; Controlled nutrient release.

Received 09 May 2025; Accepted 29 August 2025.

Introduction

Calcium phosphate nanoparticles, particularly in the form of hydroxyapatite (HAp; $Ca_{10}(PO_4)_6(OH)_2$ or $Ca_5(PO_4)_3OH$), are increasingly recognized as an innovative solution for sustainable agriculture through their application in nanoliquid fertilizers. These nanoparticles are designed to address critical challenges associated with traditional fertilizers, such as nutrient leaching, low bioavailability in alkaline soils, and inefficient phosphorus uptake by crops. Research shows that CaP nanoparticles can serve as a slow-release source of both calcium (Ca) and phosphorus (P), essential nutrients for plant growth, thus improving nutrient use efficiency and minimizing environmental impact [1]. The nanoscale size of CaP particles enhances their solubility and facilitates better plant absorption compared to bulk materials, making them particularly valuable for crops in phosphorus-deficient or alkaline soils, where traditional phosphates are less effective. Moreover, CaP nanoparticles are known to promote root and shoot growth, increase chlorophyll content, and support microbial activity in the rhizosphere, further boosting plant health and yield. In addition, studies suggest that CaP nanofertilizers can mitigate abiotic stresses, such as drought, by maintaining plant osmotic balance and enhancing root structure, which is vital for water uptake [2].

A very early study in 2011 involving the use of nano hydroxyapatite (HAp) as a Nitrogen (N) carrier through their combination with Urea (U) was provided by Kottegoda et al. and evidenced significantly slower N release by the hybrid nanostructure (Nanohybrid) compared to conventional Urea [3]. This group used a wet chemical method to evenly distribute the nano HAP from a solution of calcium hydroxide ($Ca(OH)_2$) and orthophosphoric acid (H_3PO_4) 85% with the molar ratio of Ca:P maintained at 1.67. The average size of the nano HAp was less than 100 nm in diameter.

A study by Elsayed's group in 2022 also suggested that HAp nanoparticles can release P more slowly than other types of fertilizer delivery systems while the P in nano HAp remains more mobile than the immobilized P in soil [4]. According to them, hydroxyapatite nanoparticles were synthesized based on wet chemistry from $CaCl_2.2H_2O$ solution and $NH_4H_2PO_4$ solution maintained at a ratio of 1.67. The average size of HAP nanoparticles was about 24 nm.

HAp nanoparticles were synthesized as described by Mateus et al. [5] using aqueous solutions of calcium hydroxide (Ca(OH)2), phosphoric acid (H_3PO_4), 85% and a surfactant, SDS (sodium dodecylsulphate), as starting reagents. In this experiment, Ca:P molar ratio was maintained at 1.67. The reaction takes place according to the equation:

$$6H_3PO_4 + 10Ca(OH)_2 \rightarrow Ca_{10}(PO_4)_6(OH)_2 + 18H_2O.$$

Hydroxyapatite nanoparticles obtained had different types of microspheres.

Another study by Marchiol et al. explored the potential application of HAp nanoparticles in the germination process of tomato plants [6]. They synthesized HAp nanoparticles by chemical method from H_3PO_4 solution added to $Ca(CH_3COO)_2$ solution maintaining the pH at a constant value of 10 by adding NH_4OH. The HAp nanoparticles were reported to have a size of ~50 nm as observed by TEM.

Some studies reported in the literature showed that the presence of calcium phosphate precipitation is a complex phenomenon leading to the formation of different phases: brushite, or dicalcium phosphate dehydrate (DCPD), octacalcium phosphate (OCP), hydroxyapatite (HAp) or calcium-deficient hydroxyapatite (CDHA) depending on the experimental conditions [7-9]. The main conditions influencing calcium phosphate precipitation are temperature, phosphate and calcium concentrations, pH, ionic strength and the precipitation duration [10-12]. The characteristics of calcium phosphate phases formed in different physico-chemical conditions and their chemical reactions are summarized in Table 1.

The reaction time and temperature are important factors affecting the crystallinity of the precipitating phase. The co-precipitation method for synthesizing Hydroxyurapatite in the studies of Amik Kumar Nayak et al., Bouyer E et al. and Ferraz MP et al. [14-16] requires a reaction period of 1–6 hours for precipitation, with additional aging of 12–24 hours to enhance crystallinity and phase purity, a pH typically 9–11, and reaction temperature 25–90°C.

In light of their potential benefits, CaP nanoliquid fertilizers are a promising tool for enhancing agricultural productivity and aligning with global sustainability goals, reducing dependency on large quantities of conventional chemical fertilizers and lessening nutrient runoff and soil degradation. Therefore, this report's specific tasks include synthesizing apatite nanoparticles in the presence of Triethanolamine (TEA) surfactant and analyzing their structural properties. Our group wanted to use the wet-chemical precipitation method in the presence of surfactants to conduct initial research on the application of large quantities of HAp nanoparticles with the highest uniform shape and size as fertilizer for plants.

I. Materials and Methods

All chemicals used in this study were $Ca(OH)_2$, H_3PO_4 and Triethanolamine (TEA). Calcium hydroxide ($Ca(OH)_2$, 96.0% pure) was purchased from Fisher Scientific (Honeywell Fluka, USA). Phosphoric acid (H_3PO_4, 85.0% pure) and Triethanolamine (TEA) were purchased from Petronas (Malaysia). All solutions were prepared with deionized (DI) water (18 MV cm) from a Milli-QTM Water System.

Samples of calcium phosphates were obtained by chemical precipitation from aqueous solutions. They are named 1A, 1B and 1C equivalent to three ways to prepare. The mass of the substances is taken based on the molar ratio of $Ca(OH)_2$ and H_3PO_4 being 1.5. So the masses of $Ca(OH)_2$ and H_3PO_4 are 4.73 g and 4.17 g respectively.

For sample 1A, 35 g H_2O was added to 4.73 g $Ca(OH)_2$ while stirring vigorously for about 15 minutes at 80-100 ºC. Then, cool to room temperature, 4.17 g H_3PO_4 (85%) was slowly added drop by drop to the aqueous suspension of $Ca(OH)_2$. The mixture was stirred for 1h at room temperature, obtaining a white solution with a final pH of 12 ± 0.5.

After preparing sample 1A, we added one more surfactant TEA weighing 10 g to obtain Sample 1B. The pH of Sample 1B was 11 ± 0.5 having the white suspension.

For sample 1C, we added surfactant TEA (10g) to the $Ca(OH)_2$ aqueous solution prepared at 80-100ºC. Then, lowering it to room temperature, we slowly added dropwise H_3PO_4 (4.17 g). The white solution obtained had a pH of 9.5 ± 0.05.

Table 1.

Characteristics of calcium phosphate phases with different formation conditions: molar ratio of Ca:P, pH and solubility at 25 ºC [13].

Ca/P molar ratio	Solid phase /Formula	Solubility at 25 ºC (g/L)	Formation conditions: (pH-Temperature (C))
1.0	Solid phase /Formula	~ 0.088	2.0-6.0
1.2-2.2	Dicalcium phosphate dehydrate (DCPD), mineral brushite/ $CaHPO_4.2H_2O$	Cannot be measured precisely	5-12 Always metastable
1.5–1.67	Amorphous calcium phosphates (ACPs)/$Ca_xH_y(PO4)_z.nH_2O$, n=3-4.5; 15%–20% H_2O	~ 0.0094	6.5-9.5
1.67	Calcium-deficient hydroxyapatite (CDHA)/$Ca_{10-x}(HPO_4)_x(PO_4)_{6-x}(OH)_{2-x}$ (0<x<1)	~ 0.0003	9.5-12

The white aqueous solutions of the three samples obtained were washed using de-ionized water and dried in the oven at 80°C for 24 h.

Based on the results of phase analysis and particle size distribution, the sample exhibiting the most homogeneous phase composition and the smallest particle size was selected for scale-up. The synthesis was subsequently performed at 20 times the original batch size to further evaluate the reproducibility, phase stability, and size uniformity of the HAP nanoparticles at a larger scale.

The products were characterized using X-ray Diffraction (XRD), Scanning electron microscopy (SEM), and Fourier transform infrared spectroscopy (FTIR) techniques.

The XRD patterns were recorded using the Empyrean X-ray Diffractometer from PANalytical. The data were acquired using Ni filtered copper Kα radiation in a step-by-step mode with initial 2θ =3°, final 2θ = 60°, step 2θ = 0.02°and time per step = 1.2s.

The morphology and particle size of the synthesized samples were observed using the SEM technique (FESEM, Hitachi-S4800, Japan), which is equipped with energy dispersive spectroscopy (EDS).

FTIR spectra were taken on a FTIR spectrometer (Perkin Elmer, Ltd., Buckinghamshire, UK) using KBr pellets. The discs were scanned over the range 4000 to 400 cm^{-1} with a total of 20 scans at a resolution of ±4 cm^{-1}.

The particle size distribution of the synthesized CaP nanoparticles was analyzed using a Horiba LB-550 Particle Size Analyzer, which operates based on dynamic light scattering (DLS) principles. Measurements were conducted at a fixed scattering angle of 90° and at a controlled temperature of 25°C. The instrument provided high-resolution size distribution data, allowing for the accurate determination of particle homogeneity and aggregation behavior in the suspension.

II. Results and Discussion

Figure 1 shows the flower-shaped morphology of the particles in 1A, 1B and 1C samples after synthesizing at room temperature. SEM images of 1A and 1B samples have similar morphology and particle distribution. These two samples have many particles aggregated together with sizes ranging from 50 nm to 200 nm. In the image of sample 1C, the precipitate particles are less cohesive, 30-50 nm in size as measured in Fig. 2. These flower-shaped particles are connected in a long row.

From the EDX analysis as shown in Fig. 2, the characteristic peaks of Ca, P and O are present with the atomic and weight percentages which provides the mean relative calcium to phosphate ratios as depicted in Table 2.

Table 2 represents the elemental composition of the 1A, 1B and 1C samples after synthesizing with their corresponding calcium to phosphate (Ca/P) ratios obtained by energy dispersive X-ray analysis. Weight percentage (Wt%) and atomic percentage (At%) were considered to give Ca/P approximations. From the data of Table 1, calculated Ca/P ratios in atomic (At %) for the samples 1A, 1B and 1C were 1.47, 1.52 and 1.57 respectively.

Comparatively, the atomic Ca/P ratios of three samples were close to the experimental Ca/P ratio of 1.5 for all the samples investigated in this study.

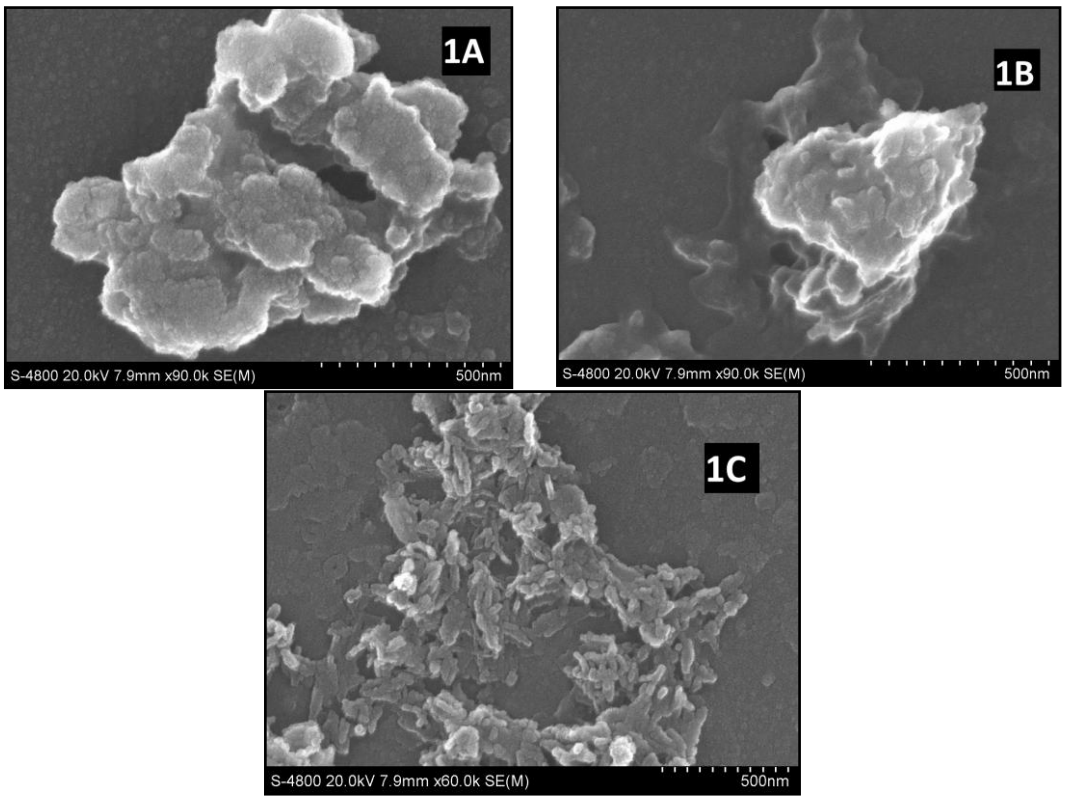

Fig.1. FE-SEM images of samples 1A, 1B and 1C.

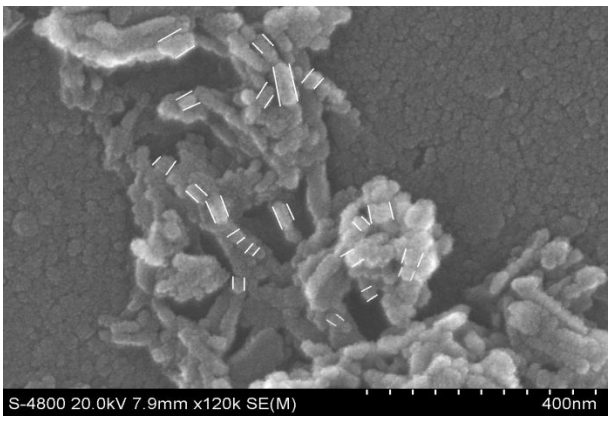

Fig. 2. FE-SEM of nanoparticles image was magnified for samples 1C.

Table 2.
Calcium/Phosphate ratios in Weight % and Atomic %.

Sample	1A	1B	1C
Calcium (Wt %)	23.13	28.84	31.99
Phosphate (Wt %)	12.22	14.64	15.78
Ca/P (Wt %)	1.89	1.96	2.02
Calcium (At %)	11.19	14.67	16.70
Phosphate (At %)	7.60	9.63	10.64
Ca/P (At %)	1.47	1.52	1.57

According to the powder X-ray diffraction (PXRD) pattern analysis shown in Figure 4 of three synthesized samples, the different phases of calcium phosphate can be obtained, depending on the experimental conditions. All three samples display the XRD patterns characterized by a baseline indicative of poorly crystalline materials. The XRD data for the precipitate particles exhibits weak and broad reflections, which were produced at room temperature through an acid-base neutralization reaction. So the presence of amorphous phases (ACp, $Ca_3(PO_4)_2.nH_2O$) alongside crystalline phases was observed in all three synthesized samples.

The pattern 1A shows a mixture of some different phase structures, however, pattern 1B shows a mixture of three phases and only one phase in pattern 1C.

XRD pattern of sample 1A reveals the presence of five phases, namely: Brushite $Ca(HPO_4)(H_2O)_2$ (JCPDS 01-072-1240); Calcium hydrogen phosphate $CaHPO_4$ (JCPDS 00-001-0653); Calcite $CaCO_3$ (JCPDS 01-086-4274); Calcium hydroxide $Ca(OH)_2$ (JCPDS 04-006-9147) (excess amount of $Ca(OH)_2$) and Hydroxyapatite (HAp) $Ca_5(PO_4)_3OH$ (JCPDS 00-001-1008). That indicates the crystallization of calcium phosphates from aqueous solutions involving some structures at a Ca/P ratio of 1.5 and pH of 12. These phase structures will always metastable for these formation conditions according to Table 1. With the conditions of Ca/P = 1.5 and pH =9-12, calcium phosphate phases in the form of Amorphous calcium phosphates (ACPs) or in the form of Calcium-deficient hydroxyapatite $(CDHA)/Ca_{10-x}(HPO_4)_x(PO_4)_{6-x}(OH)_{2-x}$ $(0 < x < 1)$ according to Table I of Sergey V. Dorozhkina [13].

However, adding surfactant TEA after preparing sample 1A to obtain sample 1B resulted in forming three phases, namely: Monetite $HCa(PO_4)$, Calcite $CaCO_3$ and

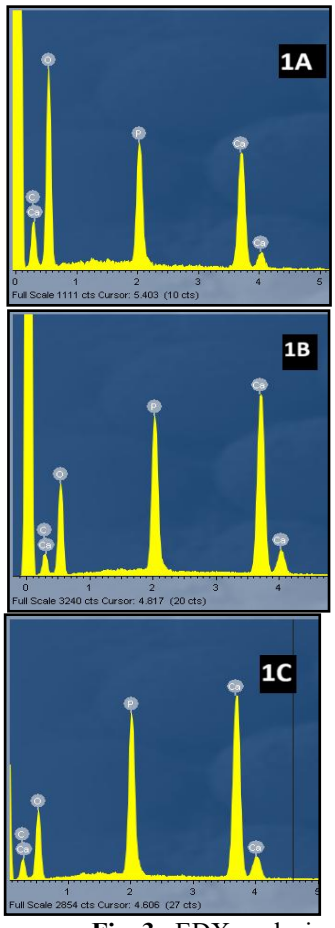

Element	Weight %	Atomic %
C	10.16	16.01
O	54.48	65.18
P	12.22	7.60
Ca	23.13	11.19

Element	Weight %	Atomic %
C	10.31	17.18
O	46.20	58.51
P	14.64	9.63
Ca	28.84	14.67

Element	Weight %	Atomic %
C	11.05	19.12
O	41.17	53.52
P	15.78	10.64
Ca	31.99	16.70

Fig. 3. EDX analysis on surfaces of 1A, 1B and 1C samples.

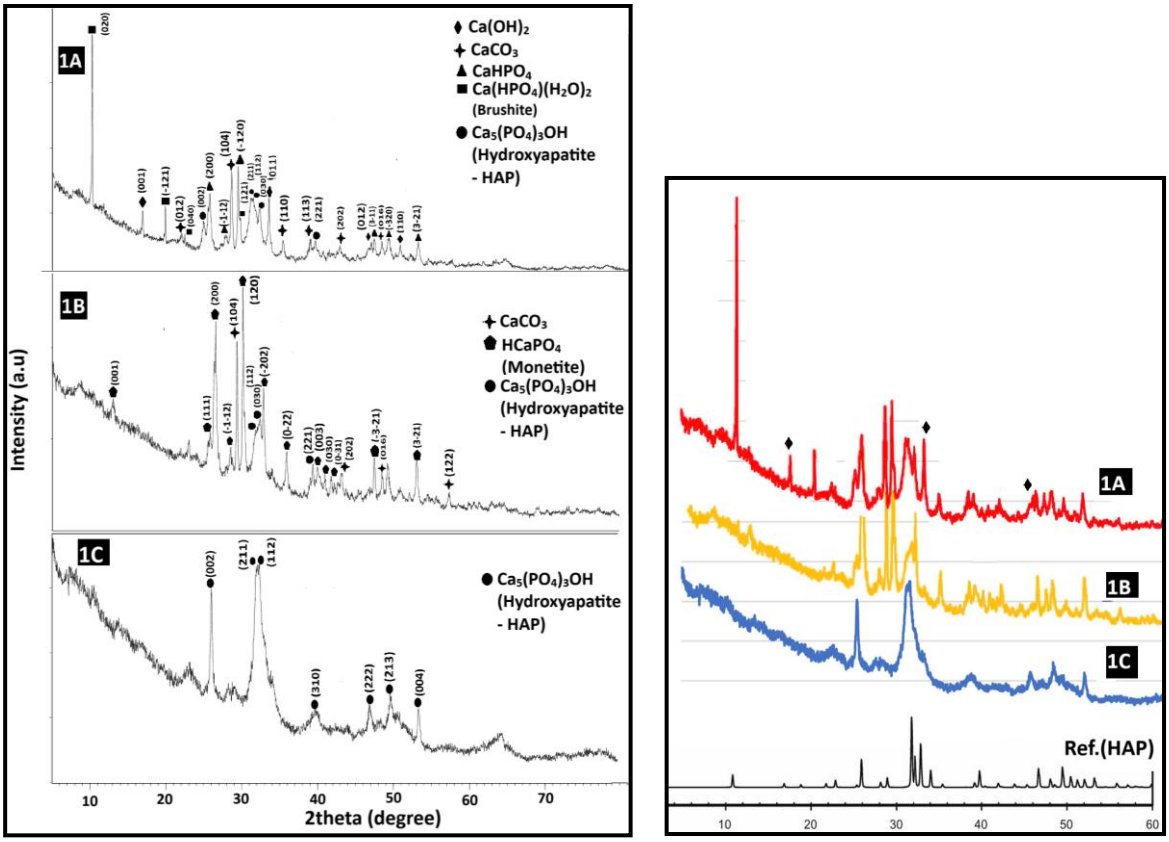

Fig. 4. Powder X-ray diffraction pattern of three samples 1A, 1B and 1C, Reference code of Hydroxyapatite: 00-001-1008.

HAp $Ca_5(PO_4)_3OH$. For sample 1C, when adding surfactant TEA to the $Ca(OH)_2$ aqueous solution prepared at 80-100 ºC and finally adding dropwise H_3PO_4, we obtained just one phase HAp. The XRD pattern of the sample 1C did not point out the presence of any phases other than HAp with all peaks matching to the JCPDS 00-001-1008 for HAp. This is in contrast to the results on the phase formation of calcium phosphate which depends on the initial crystallization conditions demonstrated in Table 1. The reaction time and temperature are also important factors which are consistent with previous studies [14-16]. The reaction time in our study is 1 hour for precipitation, with a pH of 9.5, and reaction temperature 80–100°C.

The order in which the surfactant TEA is added to the reaction solution also affects the crystallization of the phases. When TEA is added at the end of the reaction, we get three phases (in Sample 1B), but when it is added immediately after the $Ca(OH)_2$ solid solution, we get only one phase (in Sample 1C).

The crystallite size of the hydroxyapatite (HAp) sample (coded as 1C) was estimated using the Debye–Scherrer equation, which relates the broadening of diffraction peaks in the XRD pattern to the average size of crystalline domains:

$$D = (K * \lambda) / (\beta * \cos\theta)$$

Where:
- D is the average crystallite size (nm),
- K is the shape factor (typically 0.9),- λ is the X-ray wavelength (0.15406 nm for Cu Kα radiation),
- β is the full width at half maximum (FWHM) of the selected diffraction peak in radians,
- θ is the Bragg angle, i.e., half of the 2θ diffraction angle.

In this study, two prominent diffraction peaks were selected for crystallite size estimation at 2θ = 26.00° and 2θ = 32.35°, corresponding to strong reflections typically associated with HAP. The detailed crystallite sizes were calculated in Tableau 3:

Table 3.
Detailed crystallite size analysis for two prominent peaks in the XRD pattern of Hydroxyapatite (HAp) in sample 1C.

2θ (°)	FWHM (°)	Crystallite Size (nm)
26.00	0.2759	29.55
32.35	1.1167	7.41

The diffraction peak at 26.00° exhibits a relatively narrow width, indicating a larger average crystallite size of ~29.55 nm. In contrast, the peak at 32.35° is significantly broader, yielding a crystallite size of ~7.41 nm, suggesting the presence of nanocrystalline domains or amorphous character within the material.

These results confirm that the synthesized HAp sample consists of a mixture of nanocrystalline and amorphous phases, which is consistent with low-temperature synthesis routes and supports its potential application as a nano-fertilizer due to high surface area and potential bioactivity.

The FTIR (Fourier-transform infrared spectroscopy) analysis of the three samples revealed distinct functional groups of hydroxyapatite nanoparticles (PO_4^{3-}, P–O, O–P–O) (Fig. 5) [15-17].

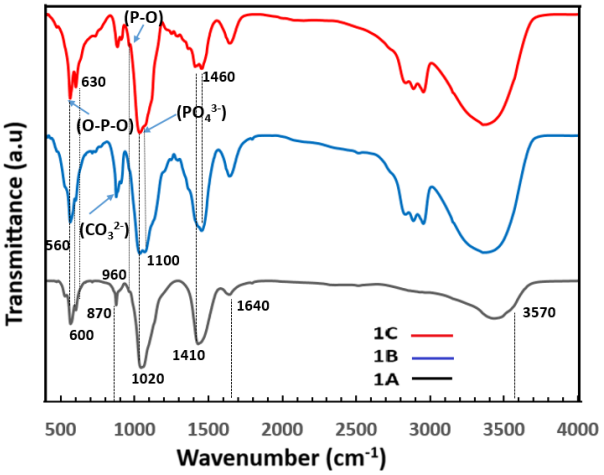

Fig. 5 Fourier Transform Infrared (FTIR) spectrum of the synthesized samples 1A, 1B and 1C.

The provided FTIR spectrum consists of three different samples (1C - red, 1B - blue, 1A - black). The characteristic functional groups of Hydroxyapatite (HAP) are identified in Table 4:

The FTIR analysis confirms the presence of functional groups characteristic of hydroxyapatite in all three samples. Sample 1A (Black spectrum) exhibits all fundamental phosphate and hydroxyl peaks, while the weak or absent carbonate peaks suggest that it is pure hydroxyapatite. Sample 1B (Blue spectrum) shows strong carbonate peaks (~870 cm^{-1}, ~1410–1460 cm^{-1}), indicating B-type carbonate substitution, where CO_3^{2-} replaces PO_4^{3-}. This composition is more similar to biological apatite found in bone mineral [18–20]. Sample 1C (Red spectrum) features sharper and more intense phosphate peaks, suggesting higher crystallinity or reduced carbonate substitution. Therefore, it is likely synthetic hydroxyapatite with high purity.

To produce a sufficient amount of material (> 1 kg) for analysis, the quantities of precursors were scaled up 20-fold compared to the initial laboratory-scale preparation. Specifically, 94.6 g of $Ca(OH)_2$ was dispersed in 700 g of deionized (DI) water under vigorous stirring at 80–100 °C. Subsequently, 200 g of triethanolamine (TEA) was added directly to the hot $Ca(OH)_2$ suspension. After cooling to room temperature, 83.4 g of H_3PO_4 (85% purity) was slowly introduced dropwise under continuous stirring. The resulting suspension was white in color and exhibited a pH of 9.5 ± 0.05.

The upscaling of sample 1C synthesis was performed to evaluate the stability, phase uniformity, and particle size distribution consistency of the hydroxyapatite (HAP) nanoparticles under near-industrial production conditions. This scale-up strategy enabled a more comprehensive assessment of the reproducibility of the chemical precipitation method and the effectiveness of TEA as both a chelating and stabilizing agent at larger batch volumes. Maintaining homogeneous dispersion, controlled particle morphology, and high crystallinity during scale-up is critical for the potential application of HAP nanoparticles in various fields, including agriculture and biomedical engineering.

For particle size measurement by dynamic light scattering (DLS), the HAP suspension of the initial laboratory-scale sample 1C was supplemented with 1.1 g of Tween 20 dispersant, corresponding to 2% of the total solution mass. For the upscaled sample 1C (20-fold increase), 22 g of Tween 20 was added to maintain the same 2% concentration relative to the total solution weight. The DLS particle size distribution of these two samples is illustrated in Figure 6.

The particle size distribution of hydroxyapatite (HAp) nanoparticles synthesized from $Ca(OH)_2$, H_2O, TEA and H_3PO_4 with Tween 20 as dispersant was measured by DLS. The results from three independent measurements consistently showed a narrow and symmetric distribution centered around 10–12 nm. The cumulative undersize curves exhibited a sharp increase, indicating a highly uniform particle size population with minimal agglomeration. The average particle size was approximately 11 nm, with negligible presence of particles larger than 100 nm. The addition of Tween 20 effectively stabilized the nanoparticles in aqueous media, preventing aggregation during synthesis and storage. The polydispersity index (PDI) was low (< 0.1), confirming the monodispersity of the suspension. These results suggest that the synthetic method produced high-purity, well-dispersed HAP nanoparticles suitable for further applications in nanotechnology and agriculture.

Table 4.

Comparative Table of Functional Groups in the FTIR Spectrum of Hydroxyapatite (HAP).

Wavenumber (cm^{-1})	Functional Group	Vibration Mode	Assignment
~560–600	PO_4^{3-}	ν_4 bending	Phosphate group (O-P-O)
~630	OH^-	Vibrational mode	Hydroxyapatite hydroxyl (-OH) group
~870	CO_3^{2-}	ν_2 out-of-plane bending	Carbonate group (A- or B-type substitution) [18-20]
~960	PO_4^{3-}	ν_1 symmetric stretching	Phosphate group in hydroxyapatite
~1020–1100	PO_4^{3-}	ν_3 asymmetric stretching	Phosphate group (P-O)
~1410–1460	CO_3^{2-}	ν_3 asymmetric stretching	Carbonate group (A- or B-type substitution) [18-20]
~3570	OH^-	Stretching	Hydroxyapatite hydroxyl (-OH) group
~ 3420 - 1640	H_2O	H-O-H bending	Adsorbed water molecules

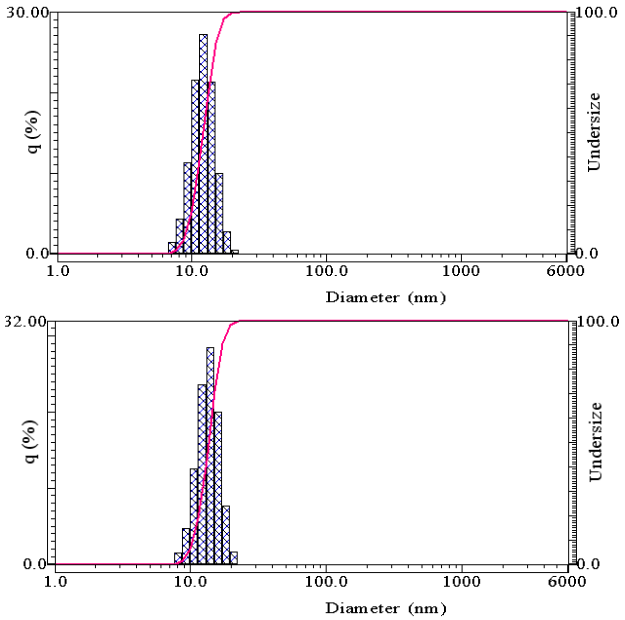

Fig. 6. Dynamic light scattering (DLS) particle size distribution of HAp nanoparticles synthesized in sample 1C: (Left) Initial laboratory-scale sample 1C, (Right) Upscaled sample 1C (20-fold increase).

The results from the SEM imaging, XRD analysis, FTIR spectroscopy, and DLS measurements of sample 1C collectively confirm the multifunctional role of triethanolamine (TEA) when introduced into the aqueous $Ca(OH)_2$ solution. TEA acts simultaneously as a chelating agent and a stabilizer during the hydroxyapatite (HAp) synthesis process, fulfilling three critical functions: (i) **Chelation:** TEA forms stable complexes with calcium ions (Ca^{2+}), regulating their availability and preventing premature precipitation, thereby enhancing uniform nucleation.
(ii) **pH Stabilization:** TEA buffers the reaction medium, maintaining a stable pH that is essential for controlled nucleation and subsequent growth of HAp crystals.
(iii) **Morphological Control:** By moderating ion activity and reaction kinetics, TEA significantly influences particle size, morphology, and crystallinity, leading to improved control over the structural characteristics of HAp.

Collectively, these mechanisms contribute to the enhanced quality, uniformity, and reproducibility of the synthesized HAp nanoparticles.

Conclusion

In this study, calcium phosphate (CaP) nanoparticles, primarily nanocrystalline hydroxyapatite ($Ca_5(PO_4)_3OH$) and amorphous calcium phosphate (ACp, $Ca_3(PO_4)_2{\cdot}nH_2O$), were successfully synthesized using a simple, cost-effective wet-chemical precipitation method. The incorporation of triethanolamine (TEA) as a chelating and stabilizing agent played a crucial role in achieving high-purity nanoparticles. TEA facilitated controlled calcium ion (Ca^{2+}) release by forming stable complexes, effectively regulating the nucleation and growth processes of hydroxyapatite. Additionally, its ability to maintain a stable pH throughout the reaction ensured excellent phase purity. TEA also influenced particle morphology, yielding uniformly shaped nanoparticles with optimal size distribution – critical for their effectiveness as nano fertilizers. This straightforward and low-cost synthesis approach provides a scalable route for producing high-purity CaP nanoparticles, offering great potential for sustainable agricultural applications.

Acknowledgments

Authors acknowledge the support of the Research Laboratories of Sai Gon Hi-Tech Park (SHTP Labs).

Compliance with Ethical Standards

The authors declare that they have no conflict of interest.

Graphical Abstract

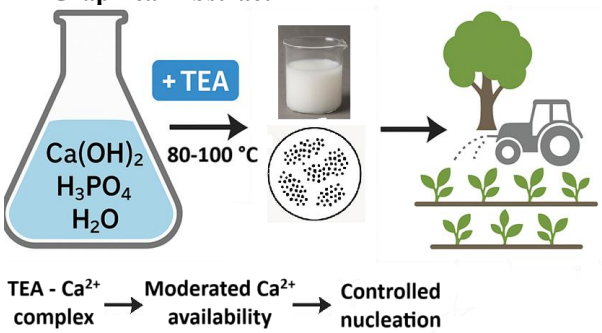

Nguyen Thi My Anh – Ph.D. in Solid State Physics, Lead Researcher at the SHTP Labs (Research Laboratories of Saigon Hi-Tech Park), specializing in nanomaterials for agriculture and sustainable energy;
Do Thanh Sinh – M.Sc. in Physical Chemistry, Research Scientist at SHTP Labs, specializing in inorganic nanomaterials and low-temperature synthesis technologies for advanced fertilizers;
Le Thai Thinh – Materials Engineer at SHTP Labs with expertise in nanostructured compounds and functional coatings for controlled nutrient release;
Nguyen Thi Kim Xuan – M.Sc. in Biotechnology and Agriculture, Researcher (focusing on the formulation of organic–inorganic nano fertilizers and biocompatible nano delivery systems for agricultural use);
Nguyen Cong Danh – M.Sc. in Physical Chemistry and Materials Science, Specialist in nanotechnology applications in soil science, with a focus on nutrient efficiency and smart fertilizer design;
Vo Nhi Kieu – M.Sc. in Organic Chemistry, Involved in research on hybrid nano fertilizers and the development of environmentally friendly nano-encapsulation techniques;
Mai Ngoc Tuan Anh – Ph.D. in Physical Chemistry and Organic Chemistry, Materials Scientist with experience in nano-structured materials for agriculture, particularly organic–inorganic hybrid nano fertilizers.

[1] Liao, Y., Xu, D., Cao, Y. et al. *Advancing sustainable agriculture: Enhancing crop nutrition with next-generation nanotech-based fertilizers.* Nano Res. 16, 13205 (2023); https://doi.org/10.1007/s12274-023-6284-8.

[2] Kamel A. Abd-Elsalam, Mousa A. Alghuthaymi, *Nanofertilizers for Sustainable Agroecosystems*, Recent Advances and Future Trends, Nanotechnology in the Life Sciences *(NALIS)*, (2024); https://www.amazon.com/dp/B0DFC39CHQ.

[3] N. Kottegoda, I. Munaweera, N. Madusanka, V. Karunaratne, *A green slow-release fertilizer composition based on urea-modified hydroxyapatite nanoparticles encapsulated wood*. Curr. Sci., 101, 73 (2011); https://www.researchgate.net/publication/269709591.

[4] A.A.A. Elsayed, A. El-Gohary, Z.K. Taha, H.M. Farag, M.S. Hussein, K. AbouAitah, *Hydroxyapatite nanoparticles as novel nano-fertilizer for production of rosemary plants*. Sci. Hortic., 295, 110851 (2022); https://doi.org/10.1016/j.scienta.2021.110851.

[5] A.Y. Pataquiva Mateus, M.P. Ferraz and F.J. Monteiro, *Microspheres based on hydroxyapatite nanoparticles aggregates for bone regeneration*, Key Engineering Materials, 330-332, 243 (2007); https://www.scientific.net/KEM.330-332.243.

[6] M. Luca, F. Antonio, A. Alessio, I. Michele, M. Alessandro, P. Elisa, D. Lorenzo, B. Enrico, *Influence of Hydroxyapatite Nanoparticles on Germination and Plant Metabolism of Tomato (Solanum lycopersicum L.),* Preliminary Evidence, Agronomy, 9, 161 (2019); https://doi.org/10.3390/agronomy9040161.

[7] Mc Dowell H., Gregory T.M., Brown W.E., *Solubility of $Ca_5(PO_4)_3OH$ in the system $Ca(OH)_2$-H_3PO_4-H_2O at 5, 15, 25, and 37 °C,* J. Res. Nat. Bur. Stand. 81, 273 (1977); https://nvlpubs.nist.gov/nistpubs/jres/081/2/V81.N02.A05.pdf.

[8] L.F. Guo, W.H. Wang, W.G. Zjang, C.T. Wang, *Effects of synthesis factors on the morphology, crystallinity and crystal size of hydroxyapatite precipitation,* J. Harbin Inst. Technol. 12, 656 (2005); https://www.researchgate.net/publication/289141451.

[9] Omar Mekmene1, Sophie Quillard, Thierry Rouillon, Jean-Michel Bouler, Michel Piot, Frédéric Gaucheron, *Effects of pH and Ca/P molar ratio on the quantity and crystalline structure of calcium phosphates obtained from aqueous solutions,* Dairy Sci. Technol. 89, 301 (2009); https://doi.org/10.1051/dst/2009019.

[10] H.E.L. Madsen, F. Christensson, *Precipitation of calcium phosphate at 40 °C from neutral solution*, J. Cryst. Growth, 114, 613 (1991); https://doi.org/10.1016/0022-0248(91)90407-V.

[11] H.E.L. Madsen, G. Thorvardarson, *Precipitation of calcium phosphate from moderately acid solution*, J. Cryst. Growth, 66, 369 (1984); https://doi.org/10.1016/0022-0248(84)90220-3.

[12] G.H. Nancollas, Z.J. Henneman , *Calcium oxalate: calcium phosphate transformations*. Urological Research. 38, 277 (2010); https://link.springer.com/article/10.1007/s00240-010-0292-3.

[13] Sergey V. Dorozhkina and Paul R. Young, *Calcium phosphates in geological, biological, and industrial systems*, In book: Water-Formed Deposits, 141 (2022); https://doi.org/10.1016/B978-0-12-822896-8.00011-X.

[14] Amit Kumar Nayak, *Hydroxyapatite synthesis methodologies: An overview*, International Journal of ChemTech Research, 2(2), 903 (2010); https://sphinxsai.com/s_v2_n2/CT_V.2No.2/ChemTech_Vol_2No.2_pdf/CT%3D24%20%28903-907%29.pdf

[15] E. Bouyer, F. Gitzhofer, MI. Boulos, *Morphological study of hydroxyapatite nanocrystal suspension.* J Mater Sci: Mater Med. 11, 523 (2000); https://doi.org/10.1023/A:1008918110156.

[16] MP Ferraz, FJ Monteiro, CM. Manuel, *Hydroxyapatite nanoparticles: A review of preparation methodologies.* J Appl Biomater Biomech. 2, 74 (2004); https://journals.sagepub.com/doi/10.1177/228080000400200202.

[17] G. Poinern, et al. *Thermal and ultrasonic influence in the formation of nanometer scale hydroxyapatite bio-ceramic*. Int. J. Nanomed. 6, 2083 (2011); https://doi.org/10.2147/IJN.S24790.

[18] M.E. Fleet. *Carbonate apatite type A synthesized at high pressure: New space group (P3̄) and orientation of channel carbonate ion*. Journal of Solid State Chemistry, 174(2), 412 (2003); https://doi.org/10.1016/S0022-4596(03)00281-0.

[19] J.C. Elliott, *Structure and chemistry of the apatites and other calcium orthophosphates.* Elsevier, Amsterdam, 1994. https://shop.elsevier.com/books/structure-and-chemistry-of-the-apatites-and-other-calcium-orthophosphates/elliott/978-0-444-81582-8.

[20] C. Rey, C. Combes, C. Drouet, and M.J. Glimcher, *Bone mineral: update on chemical composition and structure.* Osteoporosis International, 20(6), 1013 (2009); https://doi.org/10.1007/s00198-009-0860-y.

Тхі Мі Ан Нгуєн, Тхань Шінь До, Тай Тхінь Ле, Тхі Кім Суан Нгуєн,
Конг Дан Нгуєн, Ні К'єу Во, Нгок Туан Ан Май

Високочистий нано-гіроксиапатит (CaP), синтезований при низькій температурі (< 100°C): перспективний кандидат для масового виробництва нанодобрив

Дослідницькі лабораторії Саїгонського високотехнологічного парку, м. Тху Дук, м. Хошимін, В'єтнам,
ntmanh.shtp@tphcm.gov.v

Нанорідкі добрива на основі фосфату кальцію (CaP) демонструють значний потенціал у підвищенні ефективності засвоєння поживних речовин завдяки контрольованому та пролонгованому вивільненню іонів кальцію (Ca) та фосфату (P). У даній роботі було успішно синтезовано високочисті наночастинки фосфату кальцію з однорідними розмірами на рівні кількох десятків нанометрів, використовуючи простий і економічно вигідний метод. Введення триетаноламіну (TEA) як комплексоутворювального та стабілізуючого агента дало змогу суттєво знизити температуру синтезу, що зменшило енергетичні витрати та собівартість виробництва при збереженні високої якості наночастинок. Отриманий нано-гіроксиапатит ($Ca_{10}(PO_4)_6(OH)_2$) характеризується великою питомою поверхнею, що сприяє поступовому вивільненню поживних елементів та підвищеній біодоступності для рослин. Запропонований підхід забезпечує масштабовану та економічно доцільну стратегію одержання сучасних нанодобрив, орієнтованих на потреби сталого сільського господарства.

Keywords: нано-гіроксиапатит (CaP); нанодобрива; низькотемпературний синтез; триетаноламін (TEA); стале сільське господарство; контрольоване вивільнення поживних речовин.